An Optimized 3D *S*poiled Gradient for *H*emorrhage Assessment Using *IN*version Recovery and Multiple *E*choes (3D *SHINE*) for Carotid Plaque Imaging

D. C. Zhu[1], H. Ota[2], A. T. Vu[3], and J. DeMarco[2]

[1]Psychology and Radiology, Michigan State University, East Lansing, MI, United States, [2]Radiology, Michigan State University, East Lansing, MI, United States, [3]GE Healthcare, Waukesha, WI, United States

Introduction

Intraplaque hemorrhage into the carotid atherosclerotic plaque has been shown to create instability and progression. Moody et al. developed a T_1-weighted magnetization-prepared 3D gradient echo sequence to detect the hemorrhagic carotid plaque at 1.5T with a good sensitivity and specificity (1). We have also developed a similar optimized 3D inversion recovery prepared fast spoiled gradient recalled sequence (IR FSPGR) on a 3T scanner for carotid plaque imaging and have achieved a good level of success (2). Then we further enhanced the single-echo IR FSPGR, with an inclusion of multiple echo acquisitions. This sequence is called 3D SHINE (***S***poiled Gradient for ***H***emorrhage Assessment Using ***IN***version Recovery and Multiple ***E***choes) (3). The 3D SHINE sequence has been optimized in scan time, coverage and black-blood effect. With this optimized protocol, four patients with hemorrhagic carotid plaques have been studied. The T_2* values appear to be promising in characterizing the hemorrhage type (4,5). This hemorrhage type characterization may provide additional information on plaque vulnerability.

Methods

In this optimized protocol for 3D SHINE, four echoes are acquired after each RF excitation pulse at each slice phase-encoding step. By properly selecting the time of inversion (*TI*), receiver bandwidth (rBW), as well as the rest time after the sequence of slice phase encoding steps, the signal from the blood flow can be minimized to reach the maximum contrast between the carotid vessel lumen and the vessel wall. This protocol was optimized on four normal subjects and was evaluated on five patients (four with plaque hemorrhage). The data were collected on a 3T Signa® HDx MR scanner (GE Healthcare, Waukesha, WI) using a dedicated 4-channel carotid surface coil. The following optimized protocol was applied to patients (commonly with the single-echo IR FSPGR protocol): fat saturation, flip angle = 15°, field of view = 16 cm, number of slices = 40, slice thickness = 1 mm, matrix size = 256 × 192. Other parameters are shown in Table 1 below:

Table 1. Other Imaging Parameters for IR FSPGR and 3D SHINE

	rBW (kHz)	1st TE (ms)	2nd TE (ms)	3rd TE (ms)	4th TE (ms)	tr (ms)	Effect TI (ms)	Rest time (ms)	TR (ms)	Number of Excitation	Scan time
Single-echo IR FSPGR	± 31.25	3.2	None	None	None	13.7	318	0	591	2	3 min 50 sec
4-echo 3D SHINE	± 41.7	2.7	6.1	9.6	13	22.4	510	250	1208	1	3 min 54 sec

tr = time of repetition for each phase encoding step, TR = the time of repetition with respect to the non-selective inversion, and

Rest time = the extra rest time after the sequence of slice phase encoding steps.

The T_2* was calculated based on the semi-log linear regression of the voxel signal values and the corresponding *TE*s (time of echo). Specifically, $1/T_2^* = -[(\ln S_n - \ln S_m)/(TE_n - TE_m)]$, where S_n and S_m are voxel signal intensity values at *TE* values of TE_n and TE_m.

More traditional quadruple inversion-recovery T_1-weighted (6), double inversion-recovery T_2-weighted (7) and time-of-flight (TOF) images for carotid plaque imaging were also collected to confirm whether the hemorrhagic regions were Type I or II as previously validated by histological evaluation of carotid endarterectomy specimens (4,5). Single-echo IR FSPGR images with protocol shown in Table 1 were also acquired for comparison.

Regions of interests (ROI) were identified as Type I and Type II based on T_2-weighted images (4,5) and based on unbiased review by an expert reviewer. T_2* values from these ROIs were extracted. The T_2* values at the voxels of the Type I and Type II ROIs from all subjects were pooled together to calculate their distributions, and to test whether the T_2* values for Type I and Type II were statistically different from each other.

Results and Discussion

The optimized 3D SHINE sequence maintains the similar scan time as the single-echo IR FSPGR sequence. The T_2* values for Type I hemorrhage is 11.3 ± 2.9 ms and for Type II hemorrhage is 22.4 ± 8.3 ms. They are statistically different from each other ($P < 0.001$). However, when there is calcification next to the hemorrhagic region as in one of our cases, the T_2* for non-Type I hemorrhagic tissue can be reduced to the range of Type I hemorrhage and leads to false characterization. This case was excluded in the T_2* value calculated above. Fig. 1 shows results from one patient data. The hemorrhagic region can be easily identified due to its high contrast. The carotid plaque region and its associated T_2* map can be easily visualized due to the good black-blood effect and the 3D reformatting capability. Further patient evaluation is on-going. Our 3D SHINE technique appears to add great value in carotid plaque hemorrhagic detection and characterization.

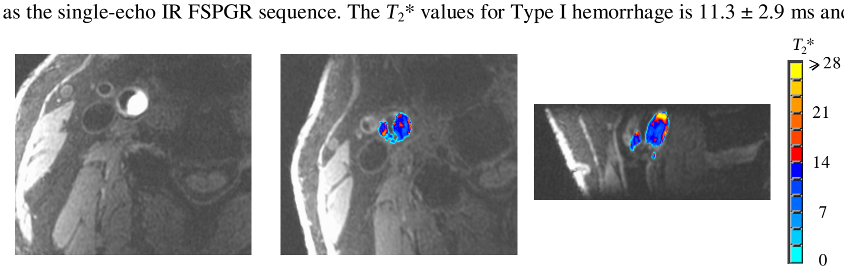

Fig. 1. The weighted average of 3D SHINE. The color-coded T_2* map can be easily visuzlied on reformated 3D SHINE images. The blue and green regions tend to be Type I hemorrhage, and the red and yellow regions tend to be Type II hemorrhage.

References

1. Moody AR, Murphy RE, Morgan PS, Martel AL, Delay GS, Allder S, MacSweeney ST, Tennant WG, Gladman J, Lowe J, Hunt BJ. Circulation. 2003;107:3047-3052.
2. Zhu DC, Ferguson MS, DeMarco JK. Magnetic Resonance Imaging. 2008 (In Press).
3. Zhu DC, DeMarco JK, Vu AT. International Society for Magnetic Resonance in Medicine, 16th Scientific Meeting and Exhibition, May 3-9, 2008, Toronto, Canada.
4. Saam T, Cai J, Ma L, Cai YQ, Ferguson MS, Polissar NL, Hatsukami TS, Yuan C. Radiology. 2006;240:464-472.
5. Chu B, Kampschulte A, Ma L, Ferguson MS, Kerwin WS, Yarnykh VL, O'Brien KD, Polissar NL,, Hatsukami TS, Yuan C. Stroke. 2004;35:1079-1084.
6. Yarnykh VL, Yuan C. Magn Reson Med. 2002;48:899-905.
7. Yarnykh VL, Yuan C. J Magn Reson Imaging. 2003;17:478-483.